

Nonequilibrium and nonlinear defect states in microcavity-polariton condensates

Ting-Wei Chen,¹ Shih-Da Jheng,² Wen-Feng Hsieh,³ and Szu-Cheng Cheng^{1,*}

¹*Department of Optoelectric Physics, Chinese Culture University, Taipei 11111, Taiwan, Republic of China*

²*Institute of Physics, National Chiao Tung University, Hsinchu 30010, Taiwan, Republic of China*

³*Department of Photonics and Institute of Electro-Optical Engineering, National Chiao Tung University, Hsinchu 30010, Taiwan, Republic of China*

(Received 16 July 2015; published 18 May 2016)

The nonequilibrium and nonlinear defect modes (NNDMs), localized by a defect in a nonequilibrium microcavity-polariton condensate (MPC), are studied. There are three analytic solutions of NNDMs in a point defect: the bright NNDM, a bound state with two dark solitons for an attractive potential, and a gray soliton bound by a defect for a repulsive potential. We find that the stable NNDMs in a nonequilibrium MPC are the bright NNDM and gray soliton bound by a defect. The bright NNDM, which has the hyperbolic cotangent form, is a bright localized state existing in a uniform MPC. The bright NNDM is a unique state occurring in a nonequilibrium MPC that has pump-dissipation and repulsive-nonlinearity characters. No such state can exist in an equilibrium system with repulsive nonlinearity.

DOI: [10.1103/PhysRevE.93.052214](https://doi.org/10.1103/PhysRevE.93.052214)

I. INTRODUCTION

Since the experimental realization of Bose-Einstein condensations (BECs) [1–3], there have been many theoretical and experimental researches devoted to nonlinear matter-wave properties of ultracold bosonic gases [4–7]. In recent years, the microcavity-polariton condensates (MPCs) created in semiconductor microcavities [8] have emerged as an attractive counterpart to the atomic BECs, owing to their intrinsically nonlinear and out-of-equilibrium nature determined by the balance between nonlinear interaction, trapping potential, pump, and dissipation [9]. The nucleation of polaritonic waves in the wake of a defect has been experimentally observed [10–12] despite a recent warning claiming that more evidence should be proposed to identify the soliton waves [13,14]. Here the repulsive polariton-polariton interactions are identified as the source of nonlinearity, which is essential for the formation of such solitary waves.

When both nonlinearity and disorder are present simultaneously, it is expected that competition between the self-action of nonlinearity and the localization induced by disorder will lead to complicated and nontrivial physical states, called *nonlinear defect modes* (NDMs). The interaction of NDMs with impurities has attracted much attention in nonlinear wave theories [15]. In these contexts, the interaction of a bright soliton with impurities has been extensively studied [16–20]. Bogdan *et al.* [17] have shown that a bright soliton state localized at a point defect in an equilibrium BEC is stable when the interaction between particles and the defect potential is repulsive and attractive, respectively. Similar conclusions were also made by analyzing localized modes supported by the generalized nonlinear Schrödinger equation with a nonlinear impurity [18,20]. These studies considered only bright solitons at a point defect and did not discuss the possible existence of dark NDMs. The interaction of a dark soliton with a localized impurity was first theoretically investigated [21] and then studied in atomic BECs [22]. After that, a variety of relevant scenarios, such as the interaction of a dark soliton

with potential steps and barriers [23,24] or with a finite-size obstacle [24,25], were also studied. All possible NDMs of the mean field of a BEC in a pointlike impurity were given in closed analytic form [26]. There are three kinds of NDMs [26]: (1) dark soliton bound by a repulsive impurity, (2) a pair of dark solitons bound by an attractive impurity, and (iii) a bright NDM with hyperbolic cotangent function solution deformed by an attractive impurity. Seaman *et al.* only described these modes and did not show under what circumstances these modes could exist. The study of self-trapping of impurities in BECs showed that the density of the BEC could increase remarkably around attractive impurities. The increased density will strongly enhance inelastic collisions between atoms in the BEC and result in a loss of BEC atoms [27].

Although nonlinearity and disorder lead to the existence of NDMs in equilibrium BECs, the study of NDMs in *nonequilibrium* MPCs is still an open area of research. Nonlinearity, nonequilibrium, and disorder can occur simultaneously in MPCs and create richer physical phenomena. The nonequilibrium character of MPCs is due to the MPCs being continuously pumped by a laser to compensate the polariton decay. As a result of interplay between nonlinearity and nonequilibrium, the incoherently pumped MPC can form vortices [28] or a vortex lattice [29] spontaneously. Differently from our preceding works focused on the finite-size pumped polaritons in a harmonic trap [30,31], we investigated the instability of a dark soliton theoretically in a homogeneous system [32]. The system is unable to support a hyperbolic-tangent dark solitons in a clean MPC [33,34]. However, under a proper repulsive disorder, the solitons could become stable.

In this paper, the overall *one-dimensional* NNDMs in MPCs under a disorder are explored by finding the solutions of the complex Gross-Pitaevskii equation coupled to the reservoir polaritons. This mean-field model for nonequilibrium MPCs is a generic model of considering effects from pumping, dissipation, defect potential, relaxation, and interactions. First, we introduce a pointlike defect into the system and find the closed analytic forms of NNDMs. We only show the symmetric wavefunctions of the system, namely, the hyperbolic-cotangent mode, bound state with two dark solitons, and gray soliton bound by a defect. Second, the numerical solutions of

*sccheng@faculty.pccu.edu.tw

the cGPE with a finite-size defect are studied in order to check the finite-size effect of a defect and confirm their dependence on the sign (attractive or repulsive) of the defect. Finally, the stability and collective-excitation spectra of NNDMs are investigated. We find that both the dark and bright solitons are stable, depending on the sign of the defect. The existence of bright solitons, which arise spontaneously due to the driven-dissipative nature of MPCs, to our knowledge has never been predicted and observed before.

II. THEORETICAL BACKGROUND

In order to study nonequilibrium MPCs, we treat the polaritons at high momenta as a reservoir whose state is determined by the reservoir density, $n_R(r,t)$. Then we employ the generalized cGPE [35], governing the condensed polaritons that couple to the reservoir polaritons, to describe the dynamics of the condensate. The wave function $\Psi(r,t)$ of the condensate and the reservoir density $n_R(r,t)$ satisfy the coupled differential equations written as

$$i\hbar \frac{\partial \Psi}{\partial t} = -\frac{\hbar^2}{2m} \frac{d^2 \Psi}{dx^2} + \frac{i}{2} \hbar [R(n_R) - \gamma] \Psi + \tilde{V}(x) \Psi + g |\Psi|^2 \Psi + 2\tilde{g} n_R \Psi, \quad (1)$$

$$\frac{\partial n_R}{\partial t} = P - \gamma_R n_R - R(n_R) |\Psi|^2, \quad (2)$$

where γ_R and γ are the decay rates of reservoir and condensate polaritons; g is the strength of polariton-polariton interaction and \tilde{g} is the coupling constant between the reservoir and condensate polaritons. $\tilde{V}(x)$ represents the external potential, and $R(n_R)$, a function of n_R , is the amplification rate that describes the replenishment of the condensate state from the reservoir state by stimulated scattering. The system is uniformly pumped with a pump power P , which will excite the reservoir polaritons.

In the steady state, the reservoir density is $n_R(x,t) = n_R^0$, and the wave function can be described by $\Psi(x,t) = \Psi_0(r) e^{-i\mu t/\hbar}$ with chemical potential μ and Planck's constant \hbar . For $P < P_{th}$ (below condensate threshold), there is no condensate density ($\Psi_0 = 0$), and the reservoir density is proportional to the pumping power, i.e., $n_R^0 = P/\gamma_R$. At the threshold, the reservoir density $n_R^{th} = P_{th}/\gamma_R$ is fixed by the balance between the amplification rate $R[n_R(x,t)]$ and decay rate γ of the condensate, i.e., $R(n_R^{th}) = \gamma$. When $P > P_{th}$, the condensate appears and the density away from the defect region, defined as $n_c = |\Psi_0|^2$, grows as $n_c = (P_{th}/\gamma)\alpha$, where $\alpha = (P/P_{th}) - 1$ is called the pump parameter being the relative pumping intensity above the condensate threshold. In the mean time, the stationary reservoir density, which is determined by the net gain being zero, is equal to the reservoir density at the threshold pump power, $n_R^0 = n_R^{th}$. Then the chemical potential of the system is $\mu = gn_c + 2\tilde{g}n_R^0$. Throughout this paper we shall take $\tilde{g} = 2g$ under the Hartree-Fock approximation. We also choose the length, time, and energy scales in units of η , $1/\omega_0$, and $\hbar\omega_0$, respectively, where $\eta = \sqrt{\hbar^2 \gamma \sigma / 2mgP_{th}}$, $\hbar\omega_0 = \hbar^2 / 2m\eta^2$, m is the polariton mass, and $\sigma = 1/[1 - (4\gamma/\gamma_R)]$. Rescaling the wave function $\Psi(x,t) \rightarrow \sqrt{n_c} \psi(x,t)$ and reservoir density

$n_R(x,t) \rightarrow n_R^{th} n(x,t)$, the cGPE of $\psi(x,t)$ and the rate equation of $n(x,t)$ are given as

$$i \frac{\partial \psi}{\partial t} = -\frac{d^2 \psi}{dx^2} + \frac{i}{2} [\tilde{R}(n) - \tilde{\gamma}] \psi + V(x) \psi + \alpha \sigma |\psi|^2 \psi + (\sigma - 1) n \psi, \quad (3)$$

$$\frac{\partial n}{\partial t} = \tilde{\gamma}_R (\alpha + 1 - n) - 4\tilde{R}(n) \frac{\alpha \sigma}{\sigma - 1} |\psi|^2, \quad (4)$$

where $\tilde{R}(n) = R(n_R)/\omega_0$, $\tilde{\gamma} = \gamma/\omega_0$, $\tilde{\gamma}_R = \gamma_R/\omega_0$, and $V(x) = \tilde{V}(x)/\hbar\omega_0$.

III. NNDMS IN A DELTA-POTENTIAL DISORDER

The solutions of Eqs. (3) and (4) with $V(x) \neq 0$ are very different from the uniform MPC. We can find analytic solutions of NNDMs if we take $V(x) = V_0 \delta(x)$, which is a pointlike potential positioned at $x = 0$. The steady state of the system under a uniform pumping can be obtained by substituting $\psi(x,t) = \psi_0(r) e^{-i\tilde{\mu}t/\hbar}$ and $n(x,t) = n_0$ into Eqs. (3) and (4), where $\tilde{\mu} = \mu/\hbar\omega_0$ is the dimensionless chemical potential of the system. For a delta-potential defect, the amplification rate $\tilde{R}(n)$ is uniform over the entire system except at $x = 0$. Therefore, the change of the amplification rate is small for a pointlike defect. We then assume that the amplification rate has no spatial dependence with $\tilde{R}(n) = \tilde{\gamma}$ in the steady state. This is, in particular, a good approximation when the decay rate of condensate polaritons is small. Equation (3) is then reduced to the standard Gross-Pitaevskii equation for an equilibrium condensate, and we can obtain the stationary reservoir density $n_0 = (\alpha + 1 - \alpha |\psi_0|^2)$ from Eq. (4). In such a steady state, there are no constant fluxes that connect the regions of loss and gain. Therefore, the densities of reservoir and the condensate polaritons can be locked together to a single time-independent nonlinear equation:

$$\tilde{\mu} \psi_0 = -\frac{d^2 \psi_0}{dx^2} + V(x) \psi_0 + \alpha |\psi_0|^2 \psi_0 + (\sigma - 1)(\alpha + 1) \psi_0. \quad (5)$$

In the region far from the defect ($x \rightarrow \pm\infty$), the densities of the system are uniform with $\psi_0 \rightarrow 1$ and $n_0 \rightarrow 1$. We then find the chemical potential of the system, $\tilde{\mu} = \alpha\sigma + (\sigma - 1)$, from Eq. (5). Substituting $\tilde{\mu}$ back to Eq. (5), we obtain

$$\frac{d^2 \psi_0}{dx^2} + \alpha(1 - |\psi_0|^2) \psi_0 = V(x) \psi_0. \quad (6)$$

When $V(x) = 0$, the solution of Eq. (6) is an unstable dark soliton [33] with a hyperbolic tangent function $\psi_0(x) = \tanh(Bx)$, where $B = \sqrt{\alpha/2}$.

We are interested in the analytical symmetric solutions of Eq. (6), and, in that case, all solutions become hyperbolic trigonometric functions with a density change around the defect and no oscillations at $x \rightarrow \pm\infty$. Such a potential models an impurity which deforms the uniform condensate on a length scale much less than the healing length of the condensate. The negative and positive values of V_0 represent attractive and repulsive impurities, respectively.

The bright NNDM, $\psi(x) = \coth[B(|x| - x_0)]$, may exist in Eq. (6), where the translational offset, x_0 , is determined by the pump parameter α and potential strength V_0 . The peak value

of $\psi(0)$ is $\coth(-x_0)$, and the density far from the maximum is approaching to unity. By integrating Eq. (6) from $-\varepsilon$ to $+\varepsilon$, and then letting $\varepsilon \rightarrow 0$, we obtain

$$\left. \frac{d\psi_0}{dx} \right|_{x=0^+} - \left. \frac{d\psi_0}{dx} \right|_{x=0^-} = V_0 \psi_0(0), \quad (7)$$

indicating that the derivative of the wave function experiences a discontinuity at the point defect. After some manipulations, we obtain

$$x_0 = \frac{1}{2B} \sinh^{-1} \left(\frac{4B}{V_0} \right). \quad (8)$$

Only the negative x_0 , corresponding to the attractive point defect, i.e., $V_0 < 0$, is valid for the *coth mode*. The positive x_0 is not allowed because it will cause a singularity at $x = x_0$.

Dark NNDMs also exist in Eq. (6) with $\psi_0(x) = \tanh[B(|x| - x_0)]$. Following the same procedure above to deal with the discontinuity of the potential around $x = 0$, now, x_0 becomes

$$x_0 = \frac{1}{2B} \sinh^{-1} \left(\frac{-4B}{V_0} \right). \quad (9)$$

The x_0 becomes positive and negative for the repulsive point defect ($V_0 > 0$) and the attractive point defect ($V_0 < 0$), respectively. Two density profiles of the dark NNDMs are available. One is the bound state with two dark solitons for $x_0 < 0$ ($V_0 < 0$), the other is the gray soliton bound by a defect for $x_0 > 0$ ($V_0 > 0$).

From the above derivations, there are three possible NNDMs of Eq. (6) depending on the sign of the defect potential: a bright NNDM [see Figs. 1(a) and 1(d)] for $V_0 < 0$, a bound state with two dark solitons for $V_0 < 0$ [see Figs. 1(b) and 1(e)], and a gray soliton bound by a defect for $V_0 > 0$ [see

Figs. 1(c) and 1(f)]. Under the pump parameter $\alpha = 1$ and the potential strength $|V_0| = 1$, the wave functions as well as the corresponding densities are shown in the first and second rows of the figure. The wave functions of NNDMs in a point defect are changing sharply around the pinning site, $x = 0$. The bright NNDM, the first solution, shows a bright localized state in a uniform MPC. The accumulation of polaritons around a defect is due to the balance of repulsive nonlinearity and attractive defect potential. The bound state with two dark solitons, the second solution, can exist under the condition that the repulsion between two dark solitons is exactly balanced by the attraction of the defect potential. The gray soliton bound by a defect, the third solution, can be treated as a single dark soliton pinned by a point defect. Here the *tanh modes* can support a notch density distribution, and the dip value of the density distribution is nonzero and given by $[\tanh(x_0)]^2$. It should be noted that the 1D spatial soliton, which could feature a localized density peak or notch accompanied by a phase jump, is pinned by the corresponding potential. The suitable terminology is a localized soliton instead of a solitary wave which is propagating.

IV. NNDMS IN A FINITE-SIZE DISORDER

After showing analytic approximation of NNDMs in a point defect, what we really want to solve is the NNDM in a finite-size defect having a Gaussian distribution. This finite-size defect, which is characterized by its strength V_d and width a , can be created by illuminating the MPC with a Gaussian beam and is given by

$$V(x) = \frac{V_d}{\sqrt{2\pi}a} e^{-\frac{x^2}{2a^2}}, \quad (10)$$

Due to the finite size of the defect, the amplification rate is modified and depends on the reservoir density. Here we assume that the amplification rate is a linear function of reservoir density, i.e., $\tilde{R}(n) = \tilde{\beta}n$ with $\tilde{\beta}$ being a constant. In the limit $x \rightarrow \pm\infty$, $\psi_0 \rightarrow 1$ and $n_0 \rightarrow 1$, we find that $\tilde{\beta} = \tilde{\gamma}$ on the steady state of the system and the chemical potential of the system is still given by $\tilde{\mu} = \alpha\sigma + (\sigma - 1)$. Applying $\tilde{R}(n) = \tilde{\gamma}n$ and $\tilde{\mu}$ to the steady states of Eqs. (3) and (4), we obtain

$$\begin{aligned} \frac{d^2\psi_0}{dx^2} - V(x)\psi_0 + \alpha\sigma(1 - |\psi_0|^2)\psi_0 - (\sigma - 1)(n_0 - 1)\psi_0 \\ - \frac{i\tilde{\gamma}}{2}(n_0 - 1)\psi_0 = 0, \end{aligned} \quad (11)$$

$$n_0(1 + \alpha|\psi_0|^2) - \alpha - 1 = 0. \quad (12)$$

Using the Newton-Raphson method, we can solve Eqs. (11) and (12) numerically. We choose the analytical solutions shown in Fig. 1 as the initial trial solutions of the Newton-Raphson method. It easily takes several iterations to get a solution correct to two decimal places. Thus the significance of the analytical work in Sec. III becomes manifest here. For $\alpha = 1$, $|V_d| = 1$, and $a = 0.5$, the wave functions as well as the corresponding condensate and reservoir densities are shown in Fig. 2. The wave functions of NNDMs in a finite-size defect are changing smoothly around the pinning site, $x = 0$. There are now only two kinds of NNDMs in a finite-size defect: a bright NNDM for $V_d < 0$ [see Figs. 2(a) and 2(c)] and a gray soliton bound by a defect for $V_d > 0$ [see Figs. 2(b) and 2(d)].

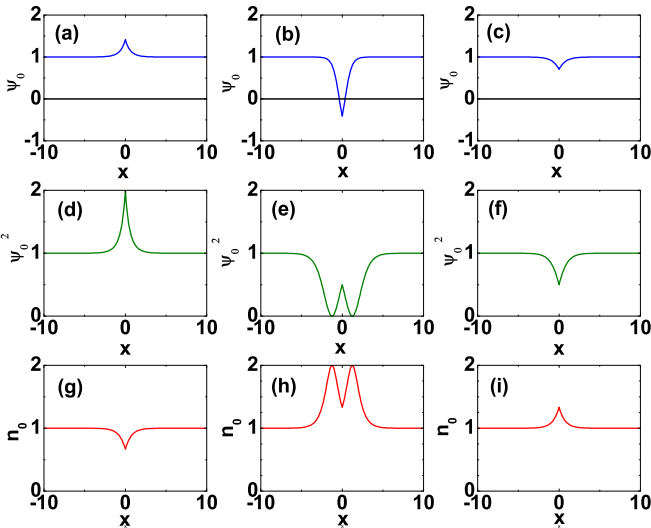


FIG. 1. Wave function $\psi_0(x)$, squared wave function $(\psi_0(x))^2$ and reservoir density n_0 of the analytical localized states. Panels (a) and (d) show the bright NNDM localized by a point defect with $V_0 = -1$; panels (b) and (e) show the bound state with two dark solitons localized by a point defect with $V_0 = -1$; and panels (c) and (f) show the gray soliton localized by a point defect with $V_0 = 1$. The pump parameter is $\alpha = 1$.

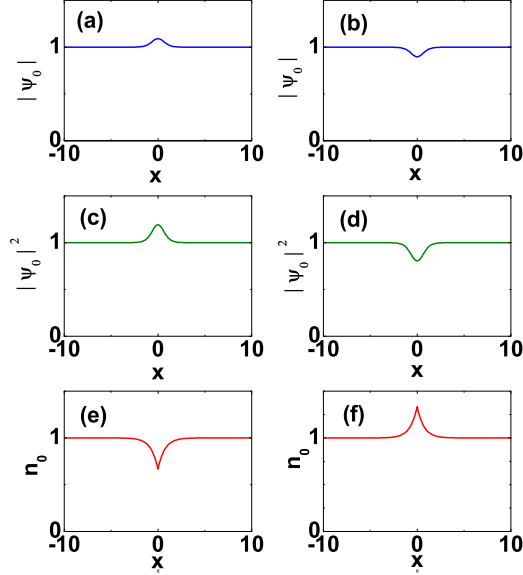


FIG. 2. Absolute wave function $|\psi_0(x)|$, squared norm $|\psi_0(x)|^2$, and reservoir density n_0 of numerical solutions for $\alpha = 1$ and $a = 0.5$. Diagrams (a), (c), and (e) are the solutions of an attractive Gaussian defect ($V_d = -1$); panels (b), (d), and (f) are the solutions of a repulsive Gaussian defect ($V_d = 1$). No solution can be found for an attractive Gaussian defect ($V_d = -1$) corresponding to the initial condition of Figs. 1(b), 1(e), and 1(h).

There is no bound state with two dark solitons for $V_0 < 0$. The numerical results confirm the analytic solutions that we have found in a pointlike defect. The bound state with two dark solitons is unstable when the polariton condensate is scattered by reservoir polaritons. With the consideration of the spatial variation of the amplification rate, the condensate density will be further decreased or increased by the accumulation or depletion of the reservoir density near the center as shown in Figs. 2(a) and 2(e) and 2(b) and 2(f).

In a *nonequilibrium* condensate under a finite defect potential, the combination of spatial inhomogeneity and pumping tend to produce states with steady state currents in order to balance the gain and loss. Since the net gain depends on local density, inhomogeneous density distributions caused by the defect imply different rates of gain or loss at different positions, so requiring currents to connect these regions. Therefore, spontaneous bright solitons [Fig. 2(c)] and gray solitons [Fig. 2(d)] are possible to be observed based on our simulation. For the case of nonresonant excitation in this work, the mechanism whereby the effective pump strength would decrease as the condensate density increases is through the consideration of a separate dynamics of the reservoir [35]. Equivalently, this introduces a *nonlinear* dissipation term modeled by Keeling *et al.* [29], which microscopically includes the depletion of reservoir density and subsequent influence of the condensate density distribution. In the typical case where the decay rates of reservoir (γ_R) or the redistribution among the different states of the reservoir is much faster than all other scales, one can adiabatically eliminate the dynamics of reservoir like Keeling *et al.* does. However, in our simulation here, $\gamma/\gamma_R = 0.2$ (or $\sigma = 5$), the consideration of reservoir density will get a more precise quantitative results.

V. BOGOLIUBOV EXCITATION SPECTRUM

We can find which NNDMs are stable from the stability analysis with a defect in the framework of the Bogoliubov-de Gennes approach [35]. We consider the steady state ψ_0 and n_0 of the system being perturbed by small fluctuations $\delta\psi$ and δn , which are given by

$$\delta\psi = u_q(x)e^{iqx}e^{-i\Omega t} + v_q^*(x)e^{-iqx}e^{i\Omega t}, \quad (13)$$

$$\delta n = w_q(x)e^{iqx}e^{-i\Omega t} + w_q^*(x)e^{-iqx}e^{-i\Omega t}, \quad (14)$$

where u_q, v_q, w_q are the amplitudes of the excitation quasiparticles, and q and Ω are the index labeling the excitation quasimomentum and frequency, respectively. The Bogoliubov spectrum then describes the energy of small wave packet with quasimomentum q on top of a macroscopically populated soliton (carrying wave) at rest. Then substituting $\psi = e^{-i\mu t}(\psi_0 + \delta\psi)$ and $n = n_0 + \delta n$ into Eqs. (3) and (4) and linearizing them around the steady state, we can obtain the excitation frequency Ω as a function of q . To linearize Eqs. (3) and (4), we have to know the functional relation between the amplification rate $\tilde{R}(n)$ and reservoir density n . For simplification we take $\tilde{R}(n) = \tilde{\beta}n$ in Eqs. (3) and (4). The decay [$\text{Im}(\Omega) < 0$] or growth [$\text{Im}(\Omega) > 0$] behavior of the excitation mode indicates the steady state of the system being stable or unstable. If the system has an eigenvalue with a positive imaginary part, the amplitude of the corresponding mode will grow exponentially in time and the mode is identified as a dynamically unstable mode.

The excitation spectra of NNDMs are shown in Fig. 3. They are respectively spectra for a bright NNDM [see Figs. 3(a) and 3(d)], spectra for a bound state with two dark solitons [see Fig. 3(b)] and spectra for a gray soliton bound by a defect

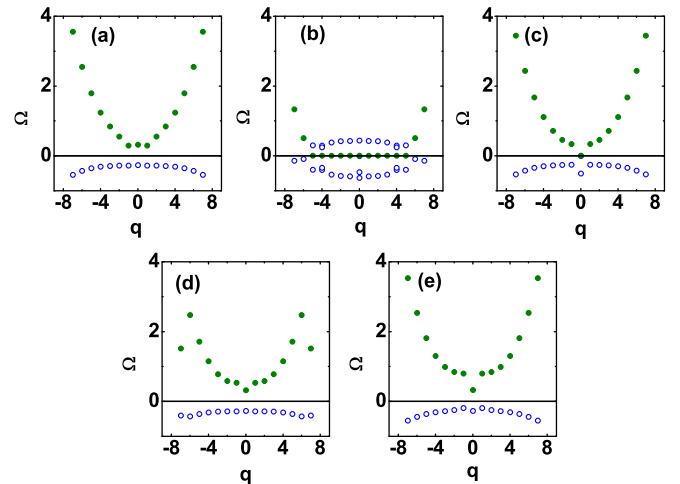


FIG. 3. The Bogoliubov excitation spectra of the lowest excitation energies corresponding to the NNDMs shown in Figs. 1 and 2. Panels (a), (b), and (c) are excitation frequencies of the bright NNDM, the bound state with two dark solitons and the gray soliton bound by a point defect, respectively. Panels (d) and (e) are excitation frequencies of the bright NNDM and the gray soliton bound by a finite-size defect, respectively. The solid and empty circles represent the real and imaginary part of the eigenvalues, respectively. The parameters: $\sigma = 5$, $\alpha = 1$, $a = 0.5$, $|V_0| = 1$, and $|V_d| = 1$.

[see Figs. 3(c) and 3(e)]. We find that the excitation energy is increasing with the momentum for the bright NNDM and gray soliton bound by a defect. From $\text{Im}(\Omega)$, we conclude that the bright NNDM and gray soliton bound by a defect are stable, but the bound state with two dark solitons by a point defect is unstable [see Fig. 3(b)] when the polariton condensate is scattered by reservoir polaritons. This is also the reason why we can not find a numerical solution for a finite defect corresponding to Fig. 1(b). For the bright NNDM, the density of the MPC is increased in the vicinity of an attractive defect. Because of the finite lifetime of polaritons, the inelastic collisions between polaritons around a defect, which is supposed to be enhanced strongly, become smaller than the equilibrium BEC. The loss of polaritons resulting from these collisions are replenished by the pump power constantly. The stabilizing mechanism of the bright NNDM is from the pump-dissipation character of nonequilibrium MPCs. The formation of the bound state of two dark solitons is a very delicate mechanism that the repulsion between two dark solitons is exactly balanced by the attraction of the defect potential. However, the balance will be destroyed if there is some density fluctuation resulting from the pump and dissipation of a nonequilibrium MPC. Then a soliton bound by two dark solitons becomes unstable and will break into two abrupt-decaying dark solitons [33]. Unlike the dark soliton, a gray soliton bound by a defect has a character that some particles exist in a dip and create repulsive forces to prevent extra particles refilling the dip. In a dip, it is difficult to redistribute the MPC density from excitations. Therefore, a gray soliton bound by a defect for $V_d > 0$ is stable. In a homogeneous-pump scheme in this work, we find that the

stable NNDMs occurring in a nonequilibrium MPC with a finite-size defect are therefore the bright NNDM [Fig. 2(a)] and gray soliton bound by a defect [Fig. 2(b)] for attractive and repulsive defects, respectively. We also notice that, for a fixed pump power, both NNDMs are stable for a wide range of defect strength.

VI. CONCLUSIONS

In summary, we study the nonlinear localized modes created by a defect in a nonequilibrium MPC. We show the analytic solutions of NNDMs for the pointlike defect and numerical solutions of NNDMs for the finite-size defects, which are pertaining to the one-dimensional MPC. There are three kinds of analytic solutions for NNDMs for a point defect: (i) a bright NNDM for an attractive defect, (ii) a bound state with two dark solitons for an attractive defect, and (iii) a gray soliton bound by a repulsive defect. However, only the bright NNDM and the gray soliton are stable in a nonequilibrium MPC. In particular, the bright NNDM shows a localized state bound by an attractive defect. The bright NNDM is a unique state occurring in a nonequilibrium MPC that owns pump-dissipation and repulsive-nonlinearity characters. There is no such state in an equilibrium BEC with repulsive nonlinearity.

ACKNOWLEDGMENTS

We acknowledge financial support from the Ministry of Science and Technology of the Republic of China under Contracts No. NSC102-2112-M-034-001-MY3 and No. NSC102-2112-M-009-016-MY3.

-
- [1] M. H. Anderson *et al.*, *Science* **269**, 198 (1995).
 - [2] J. Mattsson, *Phys. Rev. Lett.* **75**, 1678 (1995).
 - [3] K. B. Davis, M.-O. Mewes, M. R. Andrews, N. J. van Druten, D. S. Durfee, D. M. Kurn, and W. Ketterle, *Phys. Rev. Lett.* **75**, 3969 (1995).
 - [4] F. Dalfovo, S. Giorgini, L. P. Pitaevskii, and S. Stringari, *Rev. Mod. Phys.* **71**, 463 (1999).
 - [5] A. J. Leggett, *Rev. Mod. Phys.* **73**, 307 (2001).
 - [6] E. A. Cornell and C. E. Wieman, *Rev. Mod. Phys.* **74**, 875 (2002).
 - [7] W. Ketterle, *Rev. Mod. Phys.* **74**, 1131 (2002).
 - [8] J. Kasprzak *et al.*, *Nature (London)* **443**, 409 (2006).
 - [9] H. Deng, H. Haug, and Y. Yamamoto, *Rev. Mod. Phys.* **82**, 1489 (2010).
 - [10] A. Amo *et al.*, *Science* **332**, 1167 (2011).
 - [11] G. Grosso, G. Nardin, F. Morier-Genoud, Y. Léger, and B. Deveaud-Plédran, *Phys. Rev. Lett.* **107**, 245301 (2011).
 - [12] R. Hivet *et al.*, *Nat. Phys.* **8**, 724 (2012).
 - [13] P. Cilibrizzi, H. Ohadi, T. Ostatnicky, A. Askitopoulos, W. Langbein, and P. Lagoudakis, *Phys. Rev. Lett.* **113**, 103901 (2014).
 - [14] A. Amo *et al.*, *Phys. Rev. Lett.* **115**, 089401 (2015).
 - [15] Y. S. Kivshar and B. A. Malomed, *Rev. Mod. Phys.* **61**, 763 (1989).
 - [16] A. M. Kosevich, *Physica D* **41**, 253 (1990).
 - [17] M. M. Bogdan, A. S. Kovalev, and I. V. Gerasimchuk, *Low Temp. Phys.* **23**, 145 (1997).
 - [18] A. A. Sukhorukov, Y. S. Kivshar, O. Bang, J. J. Rasmussen, and P. L. Christiansen, *Phys. Rev. E* **63**, 036601 (2001).
 - [19] R. H. Goodman, P. J. Holmes, and M. I. Weinstein, *Physica D* **192**, 215 (2004).
 - [20] G. Herring, P. G. Kevrekidis, R. Carretero-Gonzalez, B. A. Malomed, D. J. Frantzeskakis, and A. R. Bishop, *Phys. Lett. A* **345**, 144 (2005).
 - [21] V. V. Konotop, V. M. Pérez-García, Y. F. Tang, and L. Vázquez, *Phys. Lett. A* **236**, 314 (1997).
 - [22] D. J. Frantzeskakis, G. Theocharis, F. K. Diakonov, P. Schmelcher, and Y. S. Kivshar, *Phys. Rev. A* **66**, 053608 (2002).
 - [23] N. G. Parker, N. P. Proukakis, M. Leadbeater, and C. S. Adams, *J. Phys. B* **36**, 2891 (2003).
 - [24] N. P. Proukakis, N. G. Parker, D. J. Frantzeskakis, and C. S. Adams, *J. Opt. B* **6**, S380 (2004).
 - [25] N. Bilas and N. Pavloff, *Phys. Rev. A* **72**, 033618 (2005).
 - [26] B. T. Seaman, L. D. Carr, and M. J. Holland, *Phys. Rev. A* **71**, 033609 (2005).
 - [27] M. Bruderer, W. Bao, and D. Jaksch, *Europhys. Lett.* **82**, 30004 (2008).
 - [28] K. G. Lagoudakis *et al.*, *Nat. Phys.* **4**, 706 (2008).
 - [29] J. Keeling and N. G. Berloff, *Phys. Rev. Lett.* **100**, 250401 (2008).

- [30] T. W. Chen, S. C. Cheng, and W. F. Hsieh, *Phys. Rev. B* **88**, 184502 (2013).
- [31] T. W. Chen, M. D. Wei, S. C. Cheng, and W. F. Hsieh, *Sol. State Comm.* **178**, 23 (2014).
- [32] T. W. Chen, W. F. Hsieh, and S. C. Cheng, *Opt. Express* **23**, 24974 (2015).
- [33] Y. Xue and M. Matuszewski, *Phys. Rev. Lett.* **112**, 216401 (2014).
- [34] L. A. Smirnov, D. A. Smirnov, E. A. Ostrovskaya, and Y. S. Kivshar, *Phys. Rev. B* **89**, 235310 (2014).
- [35] M. Wouters and I. Carusotto, *Phys. Rev. Lett.* **99**, 140402 (2007).